PHYSICAL REVIEW A **73**, 031801(R) (2006)

Experimental demonstration of high two-photon time-energy entanglement

Irfan Ali Khan and John C. Howell
Department of Physics and Astronomy, University of Rochester, Rochester, New York 14627, USA
(Received 12 January 2005; revised manuscript received 7 July 2005; published 3 March 2006)

We report on the experimental demonstration of high energy-time entanglement in two-photon states created in the process of spontaneous parametric down-conversion. We show that the classical variance product, which we violate by three orders of magnitude, actually represents a lower bound estimate of the number of information eigenmodes K. Explicit measurements estimate K to be greater than 100, with theoretical estimates predicting a value of as high as 1×10^6. These results provide incentive for the practical feasibility of large bandwidth quantum information processing, particularly in cryptography over large distances.

DOI: 10.1103/PhysRevA.73.031801 PACS number(s): 42.50.Dv, 42.65.Lm, 03.67.Mn, 03.65.Ud

Many impressive advances have been made in the field of quantum key distribution [1,2] (QKD), however, in terms of practical bandwidths and communicable distances there is still a long way to go before this technology can be used effectively for the secure communication of streaming images or other such high bandwidth applications. Recently there has been interest in developing high-dimensional entangled states for use in QKD systems due to the higher information bandwidth which would become available [3–6]. Analogous to the classical case, higher dimensionality implies greater information content per particle, which for QKD implies larger alphabets for the same particle transmission rate, as well as possibly increasing the security tolerance to noise [7,8]. Of course, for QKD these states would need to be easily transported over large distances, while at the same time preserving the entanglement. To this end photonic sources have been the medium of choice in most experimental proposals, being easily transportable over existing fiber optic networks. Additionally, the process of parametric down-conversion provides a ready source of photon pairs with a number of entangled quantum states to choose from. However, for most of these quantum states the entanglement either cannot be preserved over large distances in fiber, or the entanglement cannot be easily generalized to significantly higher dimensions [3,7,9].

Recently it was shown in Ref. [4] that by artificially discretizing the two-photon position-momentum entanglement created in down-conversion it is possible to generate D-dimensional entangled states, where D is an estimate of the number of exploitable information eigenmodes of the system. Exciting though this prospect is, the entanglement cannot be preserved over large distances using current fiber optic technology. Similar to position and momentum, energy and time are conjugate variables which obey the single particle Heisenberg uncertainty relation $(\Delta E)^2(\Delta t)^2 \geq \hbar^2/4$, also known as the time-bandwidth product, where ΔE and Δt are the measured single particle energy and time uncertainties, respectively [10]. The joint uncertainties $\Delta E_{12}=\Delta(E_1+E_2)$ and $\Delta t_{12}=\Delta(t_1-t_2)$ of two entangled particles, on the other hand, can violate the classical separability bound [11,12]

$$[\Delta E_{12}]^2[\Delta t_{12}]^2 \geq \hbar^2. \tag{1}$$

Such states are called energy-time entangled states. Some efforts have successfully used two-photon energy-time entanglement generated in the down-conversion process to perform quantum key distribution, and to generalize the scheme to higher dimensional states [5,13]. Energy-time entanglement has already been demonstrated to be well preserved over large distances and currently seems to be the most promising of the available candidates [5,13,14]. By using the ideas proposed in Ref. [4] with currently available energy-time entangled sources we show that it should be possible to generate D-dimensional entanglement with $D>100$ and possibly as high as $D\sim1\times10^6$, where the estimates are specific to our experimental parameters. In doing so, we also demonstrate an experimental violation of the classical variance product in Eq. (1) by three orders of magnitude, and show that this variance product actually represents a lower bound on the dimensionality of entanglement.

A schematic of the experiment is shown in Fig. 1. The energy-time entangled photons are created in the collinearly phasematched spontaneous parametric down-conversion process of a 2 mm long β-barium borate (BBO) crystal which is pumped by a 30 mW, cw, 390 nm laser beam. The down-converted signal and idler photons are separated from the pump by a dichroic mirror, and from each other via a polarizing beam splitter. They are then coupled into two single mode fibers. Each photon is then sent to two distinct arms of our setup (signal to arm A and idler to arm B in Fig. 1), where it is manually routed to either one arm of a Franson interferometer [15,16] or a monochromator. Using these two measurement devices we measure the two-photon coherence time and energy correlations, respectively, and hence, estimate the dimensionality of entanglement as well as the variance product. In the spirit of spacelike separated detectors we use a Franson interferometer [15] even though the same information could be obtained using the Hong Ou Mandel interferometer [17].

The Franson interferometer consists of two unbalanced Michelson interferometers, one in arm A and one in arm B. Each Michelson interferometer possesses a long and a short arm, with a time delay of τ_A and τ_B between the two arms in each Michelson, respectively. The time delays are much longer than the single photon coherence length, ensuring that no single-photon interference occurs. Additionally, this allows us to postselect long-long and short-short coincidence events, as detailed later. The time delay τ_A is varied by varying the length of the long arm in arm A with an automated

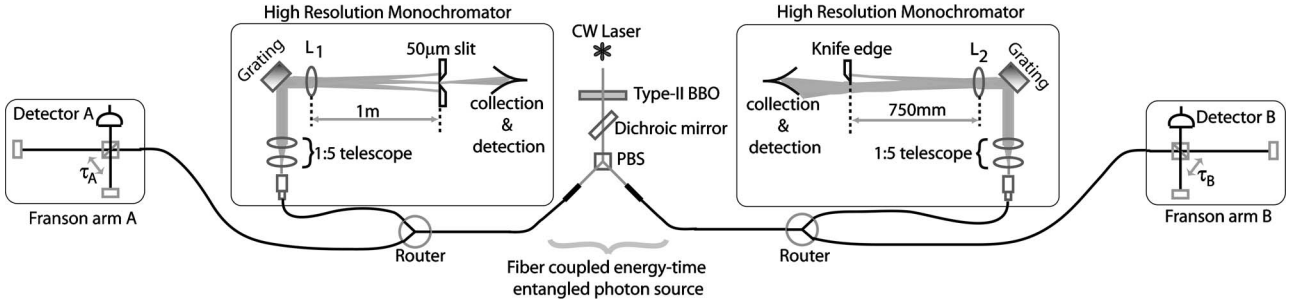

FIG. 1. Schematic of the two-photon time-energy entangled source and analyzing devices. The Franson interferometer is used to measure the biphoton coherence time, while the monochromators are used to measure an upper bound of the two-photon spectral correlations. The beam diameter of the photons in the monochromators is increased to 3.85 mm using a 1:5 telescope, then diffracted off of a diffraction grating at an incidence angle of $\sim 20°$. L_1 and L_2 are lenses of 1 m and 750 mm focal lengths respectively. τ_A and τ_B are the path mismatch in arms A and B of the Franson interferometer, respectively.

linear stage. Let us consider the expected photocoincidence rate $P(\tau_A, \tau_B)$ which is detected at the output of the Franson interferometer as a function of the time delays τ_A and τ_B [18–20]

$$P \propto \int \int |\langle 0|a_A(t_A)a_B(t_B)|\Psi\rangle|^2 dt_A dt_B, \tag{2}$$

where $|\Psi\rangle = \int \psi(t_s, t_i) e^{-i(\omega_p/2)(t_i+t_s)} a_s^\dagger(t_s) a_i^\dagger(t_i)|0\rangle dt_s dt_i$ is the biphoton wave function in the time domain, where $\psi(t_s, t_i)$ is given by

$$\psi(t_s, t_i) = \Pi\left[\frac{(t_s - t_i)}{(\pi/\Omega_f)}\right] e^{-2[\rho(t_s + t_i)]^2} \tag{3}$$

for a biphoton state generated in spontaneous parametric downconversion, $\Pi[x]$ is a rectangular function such that $\Pi[x]=1$ if $|x|<1$ and $\Pi[x]=0$ otherwise, Ω_f is half the zero-to-zero down-conversion bandwidth, ρ is the angular frequency spectrum width of the cw laser, $a_s^\dagger$ and $a_i^\dagger$ are the signal and idler creation operators, and a_A and a_B are the annihilation operators at the two detectors. In deriving Eq. (3) we have taken advantage of the fact that the cw pump has a much narrower spectrum than the phase-matching function, hence, we have already assumed that the signal and idler frequencies are anticorrelated with respect to each other about $\omega_p/2$, where ω_p is the cental pump frequency [19,21]. Consequently, the time at which the signal and idler are created in the nonlinear crystal (birth time) will be correlated to each other [19]. For the Franson interferometer, a_A and a_B can be written in terms of the signal and idler annihilation operators

$$a_A(t) = [a_s(t) + a_s(t + \tau_A)]/\sqrt{2}, \tag{4}$$

$$a_B(t) = [a_i(t) + a_i(t + \tau_B)]/\sqrt{2}. \tag{5}$$

Using the creation and annihilation operator commutation relations $[a_j(t_j), a_k^\dagger(t_k)] = \delta_{jk}\delta(t_j - t_k)$ and rejecting the long-short and short-long events through post-selection, Eq. (2) can be simplified to give

$$P(\tau_A, \tau_B) = 2 + 2\cos\left[\frac{\omega_p}{2}(\tau_A + \tau_B)\right]\Lambda\left[\frac{\tau}{(\pi/\Omega_f)}\right], \tag{6}$$

where $\Lambda[x]$ is a triangular function such that $\Lambda[x]=1-|x|$ if $|x|<1$ and $\Lambda[x]=0$ otherwise, and $\tau=\tau_A-\tau_B$. The triangular function is a result of the convolution of two square functions in this interference effect. We thus expect an oscillating fringe pattern in the measured coincidences of the Franson interferometer with a period of $4\pi/\omega_p$ and a triangular envelope of a full width at half maximum (FWHM) equal to the biphoton coherence time π/Ω_f of the down-converted photons [19,22]. The Franson interferometer therefore constitutes a nonlocal measure of the biphoton coherence time of our entangled source.

In the experiment a path mismatch of 90 cm ($\tau_{A,B} \sim 3$ ns) was used for both Michelson interferometers, much larger than the single photon coherence length of ~ 60 μm. Additionally, the acceptance window of the coincidence circuit was set at 1 ns so that we only observe long-long or short-short coincidences. We are not interested in measuring the period of the fringes, but instead in measuring the envelope over which these fringes occur which represents the correlation width of the birth time of the down-converted photons. By incrementally varying the length of the long Michelson arm in arm A it is possible to chart out the envelope of the interference pattern as shown in Fig. 2. As can be seen, the results are in excellent agreement with the theoretical envelope predicted for a zero-to-zero phase-matching width of 20 nm, which gives a biphoton coherence time of $\Delta t_{AB} = 100$ fs. The individual fringes of the interference have not been resolved since they are not central to the order-of-magnitude estimate of the envelope function. It should be noted that we measure a fringe visibility of 84% which indicates the presence of entanglement via a violation of Bell inequalities [13], however, this violation gives no quantitative information on the dimensionality of the entanglement, which is the motivation of this paper.

Next, we measure the spectral coincidence width of the signal and idler photons by routing them to the monochromators. The monochromators are set up as shown in Fig. 1, with overall spectral resolutions of ~ 0.017 nm (i.e., 8.4 GHz). By placing a 50 μm slit in the focal plane of the

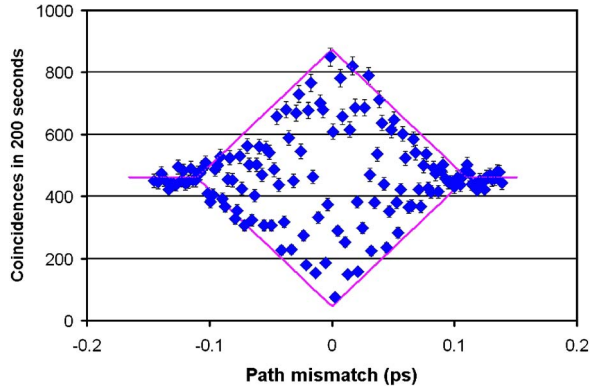

FIG. 2. (Color online) Data points depict the typical interference envelope which is observed in the coincidence rates of the Franson interferometer as a function of path mismatch. The solid line is the theoretical triangular envelope function which is calculated for a square biphoton wave function of coherence time $\pi/\Omega_f = 100$ fs.

1 m focal-length lens in arm A, we expect to create a "ghost image" of the slit in the focal plane of the 750 mm focal-length lens in arm B [11,23]. A smaller width was not chosen due to the low observed coincidence count rates. By performing a knife edge test in the focal plane of the 750 mm lens in arm B and observing coincidences we can thus measure the spectral correlations of the photons. The result of the knife edge test is shown in Fig. 3 where we measured a ghost slit width of 54 μm, which corresponds to a conditional spectral correlation width of $\Delta\lambda_A|_{\lambda_B} = 0.048$ nm ($\sim$24 GHz) [11]. We would like to stress that this measurement is not optimized since it is near the limits of the resolution of the monochromators and only represents an upper bound. The true correlation width is expected to be much less, determined by the bandwidth of the pump. We have thus measured the upper limit of the spectral correlations of the down-converted photons to be $\Delta\lambda_A|_{\lambda_B} = 0.048$ nm.

Let us reiterate what we have obtained. We have measured the *joint* birth time uncertainty (biphoton coherence time) Δt_{AB} of the entangled photons, which is relevant to the Mancini *et al.* separability criterion [11,12]. On the other hand, we have measured the *conditional* spectral uncertainty $\Delta E_A|_{E_B}$ which is relevant to the Einstein-Podolsky-Rosen (EPR) criterion [11]. We do not expect the conditional uncertainties of time and energy to vary over the range of interest. Therefore, although conditional and joint uncertainties are qualitatively different, we shall assume in our case that their measured values can be used interchangeably to reasonable approximation. Using the energy and time correlation widths measured in the experiment, we can estimate the energy-time variance product to be $(\Delta E_A|_{E_B})^2(\Delta t_A|_{t_B})^2 \sim [\Delta E_{AB}]^2[\Delta t_{AB}]^2 \sim 0.000\,22\hbar^2$, which is a three-order-of-magnitude violation of the EPR and the Mancini *et al.* separability criterion [11,12]. Although an impressive result in itself, we would like to point out that the true violation could be much stronger; the energy correlation measurement is not optimized. Using the theoretical estimate of the spectral correlation width of $\Delta\lambda_{si} \sim 5 \times 10^{-6}$ nm (calculated from a 2 MHz bandwidth servolocked pump), we would expect an optimized measurement to give a violation of the order of 11 orders of magnitude. It should be noted that these results follow through despite there being no time operator in the framework of quantum mechanics. Although this is an interesting and perhaps surprising outcome, it is not a point of contention for our results and conclusions since they can just as easily be framed in terms of longitudinal position $x_\parallel = ct$ and momentum $p_\parallel = \hbar k_\parallel = E/c$. By straightforward substitution we can obtain the familiar position-momentum uncertainty relation $(\Delta x_\parallel)^2(\Delta p_\parallel)^2 \geqslant \hbar^2/4$ and separability bound $[\Delta x_{\parallel 12}]^2[\Delta p_{\parallel 12}]^2 \geqslant \hbar^2$. We have framed this work in terms of energy and time because of the common usage of this convention in the literature.

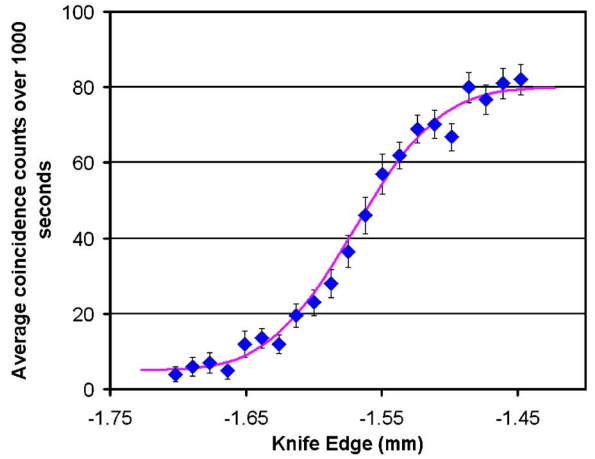

FIG. 3. (Color online) Using ghost imaging we estimate the two-photon spectral correlation width as 0.048 nm (details in text). The curve is a theoretical fit to the experimental data (squares).

Let us now consider the implications of these results when put into context of the work done in Refs. [4,24], where it is shown that the dimensionality D of entanglement is equal to the Schmidt number K of the Schmidt mode decomposition of the two-photon wave function. For a wave function of the form $\psi(t_+,t_-) = A(t_+)B(t_-)$, as in Eq. (3) where $t_\pm = t_s \pm t_i$, the Schmidt number of the decomposition can in general be shown to be given by $K \sim \frac{1}{2}(\delta t/\Delta t_{12} + \Delta t_{12}/\delta t)$, where δt and Δt_{12} are widths associated with the Gaussian-like functions $A(t_+)$ and $B(t_-)$, respectively [24]. Similarly, the Schmidt decomposition can be performed in the conjugate basis $\tilde{\psi}(E_+,E_-) = \tilde{A}(E_+)\tilde{B}(E_-)$, giving $\tilde{K} \sim \frac{1}{2}(\delta E/\Delta E_{12} + \Delta E_{12}/\delta E)$, where δE and ΔE_{12} are widths associated with the Gaussian-like functions $\tilde{B}(E_-)$ and $\tilde{A}(E_+)$, respectively. In general, because E and t are conjugate variables, it can be shown that $\delta E \Delta t_{12} \geqslant \hbar/2$ and $\delta t \Delta E_{12} \geqslant \hbar/2$. This is simply a statement of the fact that we cannot use correlation measurements to gain more information about a single particle than what is allowed by the Heisenberg uncertainty product. Using this, the Schmidt number becomes $K, \tilde{K} \geqslant \frac{1}{4}(\hbar/\Delta t_{12}\Delta E_{12})$, where the equality holds for when A and B are Gaussian functions. This is a noteworthy statement that the variance product in Eq. (1), i.e., the EPR product, is actually an estimate of the lower bound of the dimensionality of the entanglement. For our case, the variance product mea-

sured above predicts that the dimensionality of entanglement is $D \gtrsim 16$. However, since our functions are not both Gaussian, we use the measured values of the spectral widths $\delta\lambda_{dc} \sim 10$ nm and $\Delta\lambda_A|_{\lambda_B} = 0.048$ nm to obtain the more accurate estimate of $D \sim 100$. This is smaller than the estimate of $D \sim 3 \times 10^6$ obtained using the temporal widths $\Delta t_{AB} \sim 100$ fs and $\delta t \sim 300$ ns (from the 100 m pump coherence length), and therefore implies that the measured number of exploitable information eigenmodes in our source is of the order of $D \sim 100$ [4]. We would like to point out that this estimate is still low considering that we are limited by the resolution of the monochromators. The theoretical estimate of the two-photon correlation width (2 MHz) predicts that the number of eigenmodes could in reality be as high as $D \sim 1 \times 10^6$. Of course, measurements with much higher spectral resolution are required to verify this. Nevertheless, this represents a very large potential information bandwidth for quantum information applications. Especially in the realm of quantum cryptography, where evidence strongly suggests that energy-time entanglement is well preserved over very large distances in fiber [14,25], these results present an exciting prospect for immediate applicability. High dimensional cryptographic schemes have already been proposed and experimentally realized [5,26], however, this work represents the insight into the orders of magnitude of improvement which this source might be able to provide.

Considerable practical challenges still remain to be overcome before this large information bandwidth can be exploited. For example, a discrete-pixel QKD system with $D \sim 10^5$ [4] would require single photon detectors of subpicosecond timing resolution (compared with contemporary cutting edge $\sim$10 ps resolution), and monochromators of $\sim 10^{-4}$ nm spectral resolution with meters long optics and $\sim$500 nm detectors of nanosecond resolution which span an uninterupted array of $\sim$5 cm [compared with contemporary $\sim$50 μm charge coupled devices (CCDs) with microlens arrays]. However, whether through technological advancement or clever experimental construction, it is the belief of the authors that such an achievement, as motivated in this paper, would be a significant step forward in the attempt to realize a working QKD system that operates at practically desirable bandwidths.

We acknowledge A. Steinberg, J. Lundeen, J. H. Eberly, and J. D. Franson for useful discussions. J.C.H. acknowledges support from the ARO under Grant No. W911NF-05-1-0018, NSF under Grant No. EIA-0323463, ARDA under Grant No. W911NF-05-1-0197, DOD Quantum Imaging MURI, and the University of Rochester.

[1] D. Stucki, N. Gisin, O. Guinnard, G. Ribordy, and H. Zbinden, New J. Phys. **4**, 41 (2002).
[2] X. Li, P. L. Voss, J. E. Sharping, and P. Kumar, Phys. Rev. Lett. **94**, 053601 (2005).
[3] A. Mair, A. Vaziri, G. Weihs, and A. Zeilinger, Nature (London) **412**, 313 (2001).
[4] M. N. O'Sullivan-Hale, I. A. Khan, R. W. Boyd, and J. C. Howell, Phys. Rev. Lett. **94**, 220501 (2005).
[5] H. de Riedmatten, I. Marcikic, V. Scarani, W. Tittel, H. Zbinden, and N. Gisin, e-print quant-ph/309058 (2004).
[6] L. Neves, G. Lima, J. G. Aguirre Gomez, C. H. Monken, C. Saavedra, and S. Padua, Phys. Rev. Lett. **94**, 100501 (2005); M. P. Almeida, S. P. Walborn, and P. H. Souto Ribeiro, Phys. Rev. A **72**, 022313 (2005).
[7] H. Bechmann-Pasquinucci and W. Tittel, Phys. Rev. A **61**, 062308 (2002).
[8] N. J. Cerf, M. Bourennane, A. Karlsson, and N. Gisin, Phys. Rev. Lett. **88**, 127902 (2002).
[9] T. Jennewein, C. Simon, G. Weihs, H. Weinfurter, and A. Zeilinger, Phys. Rev. Lett. **84**, 4729 (2000).
[10] A. Messiah, *Quantum Mechanics* (Dover, Mineola, NY, 1999).
[11] J. C. Howell, R. S. Bennink, S. J. Bentley, and R. W. Boyd, Phys. Rev. Lett. **92**, 210403 (2004).
[12] S. Mancini, V. Giovannetti, D. Vitali, and P. Tombesi, Phys. Rev. Lett. **88**, 120401 (2002).
[13] W. Tittel, J. Brendel, H. Zbinden, and N. Gisin, Phys. Rev. Lett. **84**, 4737 (2000).
[14] W. Tittel, J. Brendel, H. Zbinden, and N. Gisin, Phys. Rev. Lett. **81**, 3563 (1998).
[15] J. D. Franson, Phys. Rev. Lett. **62**, 2205 (1989).
[16] P. G. Kwiat, A. M. Steinberg, and R. Y. Chiao, Phys. Rev. A **47**, R2472 (1993).
[17] C. K. Hong, Z. Y. Ou, and L. Mandel, Phys. Rev. Lett. **59**, 2044–2046 (1987).
[18] J. G. Rarity and P. R. Tapster, Phys. Rev. A **45**, 2052 (1992).
[19] V. Giovannetti, L. Maccone, J. H. Shapiro, and N. C. Wong, Phys. Rev. A **66**, 043813 (2002).
[20] O. Kuzucu, M. Fiorentino, M. A. Albota, N. C. Wong, and F. X. Kärtner, Phys. Rev. Lett. **94**, 083601 (2005).
[21] W. P. Grice and I. A. Walmsley, Phys. Rev. A **56**, 1627 (1997).
[22] T. B. Pittman, D. V. Strekalov, A. Migdall, M. H. Rubin, A. V. Sergienko, and Y. H. Shih, Phys. Rev. Lett. **77**, 1917 (1996).
[23] M. Bellini, F. Marin, S. Viciani, A. Zavatta, and F. T. Arecchi, Phys. Rev. Lett. **90**, 043602 (2003).
[24] C. K. Law and J. H. Eberly, Phys. Rev. Lett. **92**, 127903 (2004).
[25] I. Marcikic, H. de Riedmatten, W. Tittel, H. Zbinden, M. Legre, and N. Gisin, Phys. Rev. Lett. **93**, 180502 (2004).
[26] R. T. Thew, A. Acin, H. Zbinden, and N. Gisin, Phys. Rev. Lett. **93**, 010503 (2004).